

## ON THE METHOD TO INFER AN ATMOSPHERE ON A TIDALLY LOCKED SUPER EARTH EXOPLANET AND UPPER LIMITS TO GJ 876d

S. SEAGER<sup>1</sup> AND D. DEMING<sup>2</sup>

<sup>1</sup> Department of Earth, Atmospheric and Planetary Sciences, Department of Physics, Massachusetts Institute of Technology,  
77 Massachusetts Ave., Cambridge, MA 02139, USA

<sup>2</sup> Planetary Systems Branch, Code 693, NASA/Goddard Space Flight Center Greenbelt, MD 20771, USA

Received 2008 November 28; accepted 2009 August 6; published 2009 September 15

### ABSTRACT

We develop a method to infer or rule out the presence of an atmosphere on a tidally locked hot super Earth. The question of atmosphere retention is a fundamental one, especially for planets orbiting M stars due to the star's long-duration active phase and corresponding potential for stellar-induced planetary atmospheric escape and erosion. Tidally locked planets with no atmosphere are expected to show a Lambertian-like thermal phase curve, causing the combined light of the planet–star system to vary with planet orbital phase. We report *Spitzer* 8  $\mu\text{m}$  IRAC observations of GJ 876 taken over 32 continuous hours and reaching a relative photometric precision of  $3.9 \times 10^{-4}$  per point for 25.6 s time sampling. This translates to a  $3\sigma$  limit of  $5.13 \times 10^{-5}$  on a planet thermal phase curve amplitude. Despite the almost photon-noise-limited data, we are unable to conclusively infer the presence of an atmosphere or rule one out on the non-transiting short-period super Earth GJ 876d. The limiting factor in our observations was the miniscule, monotonic photometric variation of the slightly active host M star, because the partial sine wave due to the planet has a component in common with the stellar linear trend. The proposed method is nevertheless very promising for transiting hot super Earths with the *James Webb Space Telescope* and is critical for establishing observational constraints for atmospheric escape.

*Key words:* planetary systems – stars: individual: (GJ 876) – techniques: photometric

*Online-only material:* color figures

### 1. INTRODUCTION

Super Earths are a recently discovered class of exoplanets, loosely defined to be  $10 M_{\oplus}$  or less. Since these planets have low masses, they likely consist substantially of rocky material, making them the first analogs of terrestrial planets in our solar system. The search for super Earths around G through M stars continues (e.g., Baglin 2003; Borucki et al. 2003; Butler et al. 2004; Bonfils et al. 2007; Endl & Kürster 2008; Nutzman & Charbonneau 2008; Mayor et al. 2009), with many discoveries of transiting super Earths (Leger et al. 2009) anticipated in the next few years.

A fundamental question about rocky planets is whether or not they have an atmosphere. The atmosphere can regulate the temperature and protect the surface from harmful solar or cosmic rays, issues central to surface habitability. Extreme ultraviolet (EUV) radiation, winds, and coronal mass ejections (CMEs; Lammer et al. 2007) from the host star are the main mechanisms for driving atmospheric escape. M stars have a much longer active phase compared to solar-like stars, during which a star's EUV, winds, and CMEs are strong (Scalo et al. 2007; West et al. 2008). The issue of atmospheric retention, therefore, is especially relevant for super Earths in short-period orbits around M stars (e.g., Lammer et al. 2007).

We are motivated to observationally determine whether or not a tidally locked close-in super Earth orbiting an M star has an atmosphere. The goal is to observe the planet and star in combined light and search for thermal phase variations peaking at the substellar point, indicative of a bare rock planet with no atmosphere.

The idea to study transiting hot super Earths in this way was briefly mentioned in Selsis (2004) and Nutzman & Charbonneau (2008). On a related topic, Gaidos & Williams (2004) and Selsis (2004) developed the same idea for non-transiting terrestrial

planets orbiting at the Earth's semi-major axis from a Sun-like star. The idea would be to use a Terrestrial Planet Finder/Darwin-type interferometer (e.g., Cockell et al. 2009; Lawson et al. 2008, and references therein) to null out the star light to directly image the planet over the course of its orbit. Gaidos & Williams (2004) explored light curves of planets with and without atmospheres and oceans, for a variety of obliquities, eccentricities, and viewing geometries. Combined light-phase curves of about half a dozen hot Jupiter transiting planets have been obtained with the *Spitzer Space Telescope* (e.g., Harrington et al. 2006; Cowan et al. 2007; Knutson et al. 2007, 2009). Even though our first proposal to observe a hot super Earth phase curve was in 2005, three attempts at observations were needed to reach a reasonable S/N and to mitigate instrument systematics.

We begin in Section 2 with a description of the motivation and background to detect an atmosphere on a tidally locked super Earth. In Section 3, we describe *Spitzer* IRAC observations of the planet-hosting M dwarf star GJ 876A and report on upper limits to inferring an atmosphere on the short-period super Earth GJ 876d. In Section 4, we discuss prospects for the method to infer or rule out an atmosphere on tidally locked super Earths, including transiting exoplanets.

### 2. MOTIVATION AND BACKGROUND

The motivating factor for observations to discriminate between a bare rock and a planet with an atmosphere is simply that basic atmospheric escape estimates and calculations are inconclusive because they are highly dependent on assumed planetary parameters (such as mass, primordial atmosphere mass, and the past EUV radiation history of the host star).

Atmospheric escape is a complex process thought to be driven by nonthermal escape processes or by EUV radiative heating. The high temperatures and consequent expanding

upper atmosphere enable thermal escape of gases. To illustrate the main uncertainties in EUV heating, we use the energy-limited escape framework (Lecavelier des Etangs 2007). The gravitational potential energy of the planet [J] is

$$E_p = -\frac{GM_p m_{\text{atm}}}{\beta R_p}, \quad (1)$$

where  $G$  is the gravitational constant,  $M_p$  is the planet mass,  $R_p$  is the planet radius, and  $\beta R_p$  is the radial extent of the planet exosphere. Here  $m_{\text{atm}}$  is the mass of the planet atmosphere, which we assume to be low enough to ignore the radial atmosphere structure in our estimate. The incident EUV power [ $\text{J s}^{-1}$ ] incident on the planet is

$$P_{UV} = \pi R_p^2 F_{\text{EUV}}. \quad (2)$$

We assume here that the radius where the EUV energy is absorbed is close enough to the planetary radius. Taking the ratio of Equations (1) and (2), and an active-phase average EUV flux ( $F_{\text{EUV}}$ ) leads to the lifetime of the initial planet atmosphere

$$\tau \sim \left[ \frac{G}{\pi} \right] \left( \frac{M_p}{R_p^3} \right) \frac{m_{\text{atm}}}{\beta \epsilon \langle F_{\text{EUV}} \rangle}. \quad (3)$$

Energy-limited escape assumes that some fraction,  $\epsilon$  of the incident UV flux heats the atmosphere and drives escape. Note that  $\beta > 1$  and  $\epsilon < 1$ . This equation is valid provided that the upper atmosphere is heated strongly enough for the relevant elements (e.g., H, or C) to escape.

We can see the main uncertainties in atmospheric thermal escape from Equation (3), even though the equation is approximate at best. First, if a planet is transiting we know the planetary density. If the planet is not transiting and we assume the planet is solid, the density varies by less than a factor of 5 for reasonable interior compositions (Mercury-like to a “dirty water” planet) and for a range of planetary masses (e.g., Seager et al. 2007). More uncertain is the initial outgassed planetary atmosphere mass, which could vary widely, from less than 1% of the planet’s total mass up through 5% and even as high as 20% for an initially water-rich planet (Elkins-Tanton & Seager 2008). An equally large unknown is the incident EUV flux. All stars have very high EUV flux during their so-called “saturation phase,” where levels can reach thousands of times present-day solar EUV levels. The high EUV is most critical for planets orbiting M stars: M star saturation phases can last 1–3 billion years for early M stars and 6–8 billion years for late M stars (M5–M8; West et al. 2008). If the initial planetary atmosphere has not survived during the star’s saturation phase, a new atmosphere could develop in the star’s quiet phase if the outgassing rate is higher than the escape rate.

The basic idea for observations is that a tidally locked planet with no atmosphere, i.e., a bare rock, will show a thermal phase variation that can be observed in the combined light of the planet–star system. We assume that short-period super Earths are tidally locked based on dynamical timescales (Goldreich & Soter 1966).

As long as the temperature is high enough, the absorbed stellar radiation is approximately instantaneously reradiated on a bare rock planet. We can see this in a first order way by comparing the radiative flux to the conductive flux. The radiative flux is

$$F_R = \sigma T^4, \quad (4)$$

where  $\sigma$  is the radiation constant  $\sigma = 5.670 \times 10^{-8} \text{ J K}^{-4} \text{ m}^{-2} \text{ s}^{-1}$ . Conduction is in general very inefficient in rocky material. Heat conduction is defined by

$$F_C = \frac{dQ}{dt dA} = -k \frac{dT}{dz}, \quad (5)$$

where  $Q$  is heat,<sup>3</sup>  $A$  is the cross-sectional heating area,  $dQ/dt dA$  is the heat flux,  $k$  in units  $\text{W m}^{-1} \text{ K}^{-1}$  is the thermal conductivity. For Earth’s surface materials,  $k \sim 3$ . Conduction describes how heat is transferred from a hotter to a colder region, as indicated by the negative temperature gradient in the above equation.

We can estimate the conductive flux by adopting different temperature gradients  $dT/dz$ . A tidally locked planet has a maximum temperature gradient across the surface created by the drop off of incident stellar flux away from the substellar point. This drop-off follows  $(1 - \cos \theta)^{1/4}$ , where  $\theta = 0$  is defined at the substellar point and  $\theta$  is the angle away from the substellar point surface normal, and using Equation (4). The temperature change across 10 m, 100 m, or even 1 km is much less than a fraction of a percent. The same line of reasoning can be applied to regions away from the substellar point, also resulting in the dominance of radiation over conduction. Hence the conductive flux across the surface is essentially negligible, and radiation back to space will dominate over conduction away from the heated surface element.

We can also estimate the conductive flux from the surface down into the planet interior. We can conservatively take Earth’s subsurface temperature; a more massive planet is likely to be hotter in the subsurface due to more heat-generating radioactive decay, and tidal heating may also play a role. The Earth’s subsurface temperature at a depth of 500 m is about 293 K. This is deep enough so that the primary heat source is radioactive decay of elements in the Earth’s interior. If we take GJ 876’s substellar temperature of  $\sim 650$  K, then, using Equations (4) and (5), the radiative flux is 5000 times greater than the conductive flux, showing that radiation back to space will dominate over conduction of energy down into the planetary interior. Even if we take an artificially extreme case of a  $10 \text{ K m}^{-1}$  temperature gradient just beneath the planet’s surface, the radiative flux is still a few hundred times greater than the conductive flux. We note that Earth is hotter in the interior than at the surface and has a temperature gradient of about  $0.02\text{--}0.03 \text{ K m}^{-1}$ ; on Earth there is no conduction of absorbed sunlight down into the crust because conduction only operates from hotter to colder regions.

In summary, as long as the temperature is high enough, reradiation will dominate over conduction. We may say that if a hot super Earth is hot enough for its atmosphere to have escaped, it should also be in a regime where reradiation dominates over conduction. Gaidos & Williams (2004) have used a different line of reasoning to argue that the thermal inertia of even cooler rocky planets is negligible.

For instantaneous absorption and reradiation, the planetary thermal phase curve for a tidally locked bare rock takes the same expression as that of a Lambert sphere (Sobolev 1975),

$$\Phi_\alpha = \frac{1}{\pi} [\sin \alpha + (\pi - \alpha) \cos \alpha]. \quad (6)$$

The phase angle,  $\alpha$ , is the star–planet–observer angle. With this definition,  $\alpha = 0^\circ$  corresponds to “full phase,”  $\alpha > 170^\circ$

<sup>3</sup>  $Q$  is heat in the form of kinetic energy of the motion of atoms and molecules.

corresponds to a thin crescent phase, and the planet is not at all illuminated at  $\alpha = 180^\circ$ . The phase angle in terms of inclination is

$$\cos \alpha = -\sin i \sin 2\pi \phi, \quad (7)$$

where  $\phi$  is the orbital phase. For the phase-dependent thermal infrared flux ratio of a bare rock, we have an expression similar to that of reflected light (e.g., Sobolev 1975; Charbonneau et al. 1999) with the geometric albedo  $A_g$  replaced by  $(1 - A_g)$ ,

$$\frac{F_p(\phi, i)}{F_*} = (1 - A_g) \left(\frac{R_p}{a}\right)^2 \frac{1}{\pi} [\sin \alpha + (\pi - \alpha) \cos \alpha]. \quad (8)$$

We are therefore looking for a sinusoidal variation like a Lambert sphere, depending on the inclination of the planet. Detection of a Lambertian thermal phase curve is a necessary but not sufficient condition to identify a tidally locked exoplanet without an atmosphere. Some tidally locked exoplanet atmospheres, including those with thin atmospheres or with strong absorbers at high altitudes in thick atmospheres will show a thermal phase curve that peaks on the planetary day side. The only way to discriminate between a tidally locked bare rock exoplanet and tidally locked planet with a thin or thick atmosphere is that atmospheric winds likely shift the planetary hot spot away from the substellar point. The data need to be good enough to pinpoint the hottest point on the planetary day side to see whether or not it is consistent with the substellar point.

### 3. OBSERVATIONS AND DATA ANALYSIS

We observed GJ 876d, because at the time of our first proposed observations (2005) GJ 876d was the only short-period super Earth candidate available for the method to infer the presence of an atmosphere. GJ 876 (Rivera et al. 2005) is a dM4 star with  $T_{\text{eff}} = 3350 \pm 300$  K (Maness et al. 2007). At a distance of 4.69 pc, GJ 876 is a nearby star and very bright in the near-IR ( $K = 5.0$ ).

The planet GJ 876d has  $M \sin i = 5.89 \pm 0.54 M_\oplus$ ,  $P = 1.93776 \pm 7 \times 10^{-5}$ , and a semi-major axis of 0.02 AU (Rivera et al. 2005). A non-transiting planet, GJ 876d's orbital inclination is unknown. Despite being a relatively slow rotator (96<sup>d</sup>.7 period; Rivera et al. 2005), and relatively inactive, GJ 876 has a low-level brightness variability of order 0.05 mag at visible wavelengths (Shankland et al. 2006).

We observed GJ 876 at  $8 \mu\text{m}$  wavelength using *Spitzer*/IRAC. The observations were nearly continuous for 32 hr, starting on 2008 July 16 at 01:50 UTC, using an Instrument Engineer Request in two segments. We acquired a total of 4204 data cubes in IRAC subarray mode, each data cube comprising 64 exposures of 0.4 s duration, and  $32 \times 32$  pixel spatial extent. IRAC observations at  $8 \mu\text{m}$  are subject to an increasing sensitivity as the detector is exposed to light, an effect termed the ‘‘ramp’’ (Deming et al. 2006). We used a ‘‘pre-flash’’ strategy to flood the detector with high flux levels and thus force the ramp to its asymptotic value prior to observing GJ 876: we observed the compact H II region WC89 for 59 minutes immediately prior to observing GJ 876.

Our analysis used the Basic Calibrated Data produced by version S18.0.2 of the *Spitzer* analysis pipeline. We applied the corrections recommended by the *Spitzer Science Center* (SSC) to correct for variations in the pixel solid angle and flat-fielding for point sources. We corrected the effect of energetic particle hits by applying a five-point median filter to the 64-frame time history of each pixel within each data cube. We

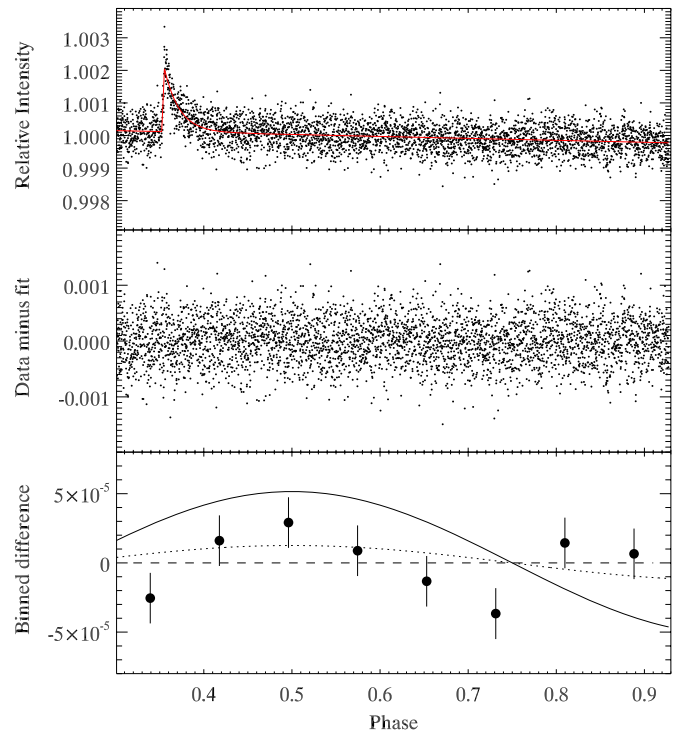


**Figure 1.** Upper panel: photometry of GJ 876 for 3828 data cubes, each representing 62 images. The initial small detector ramp, represented by 376 data points (159 minutes) was omitted from the analysis and is not shown. The red line is a fit of a linear (0.002 per day) brightness decrease of the star, plus a flare of amplitude 0.002 near phase 0.355. Middle panel: data from the upper panel after the fit (red line) is subtracted. Lower panel: residuals from the middle panel binned into 8 phase intervals, and shown in comparison to our  $3\sigma$  upper limit on the flux modulation (solid curve, amplitude =  $5.13 \times 10^{-5}$ ,  $44 \mu\text{Jy}$ ) peaking at phase 0.5 as expected for a planet without an atmosphere to redistribute heat. The dotted curve is the nominal best fit (not a detection).

(A color version of this figure is available in the online journal.)

set the threshold of the median filter to equal 6% of the peak value in the average stellar image, and we corrected discrepant pixels to the median value. We performed aperture photometry on each of the 64 frames within each data cube, using a circular aperture with a radius of 4.25 pixels. We centered the aperture for each frame using a parabolic fit to the brightest 3 pixels in the X- and Y-profiles of the star, each profile derived by summing over the orthogonal coordinate. We varied the aperture radius to minimize the scatter in the final photometric time series. We measured a background value using an annulus with inner and outer radii of 6 and 12 pixels. Each photometric point (Figure 1) was constructed by averaging the frames within each data cube, omitting the first and 58th frame (see Harrington et al. 2007). We also omitted frames that were internally discrepant by more than  $4\sigma$  from the other frames within each data cube. We subtracted an average background value for the entire time series (not frame by frame) because this minimized the scatter in the time series photometry.

Figure 1 (top panel) shows the photometric time series. We found that a very small ramp effect (about 0.1%, not illustrated in Figure 1) was still present for the first  $\sim 2$  hr of the data. We simply dropped the first 159 minutes of data from the analysis, keeping the last 3828 data cubes (orbit phases  $\geq 0.3$ ).

The most prominent feature in Figure 1 is a 2 mmag stellar flare that occurs near phase 0.355. Flares are quite common on active M dwarfs (Reid & Hawley 2005), although none have been previously reported on GJ 876. However, three facts

indicate that this is a real flare: (1) *Spitzer* photometry for solar-type stars has a proven stability (e.g., Knutson et al. 2007), with no instrumental effects of this type; (2) the event has the characteristic rapid rise and exponential decline characteristic of M dwarf flares; and (3) Knutson et al. (2007) and H. Knutson et al. (2008, private communication) observed a similar event on the M dwarf companion to HD 189733. We fit and remove a flare model from the photometry. The flare model has a linear rise and exponential decline, requiring four parameters (rise rate, time of peak, amplitude, and decay rate), and we fit for the minimum  $\chi^2$  using a gradient-expansion algorithm. We emphasize that the flare is not a significant impediment to our analysis, because it has a well-defined shape and occupies only a relatively small fraction of the light curve.

In addition to the flare, we observe a gradual decline in brightness that is equivalent to 0.6 mmag per day. GJ 876 is known to be variable (Weis 1994), and ground-based photometry in the Johnson *B* band by P. Sada (2008, private communication) for times bracketing our *Spitzer* observations shows a decrease in brightness at a rate of  $2.0 \pm 0.2$  mmag per day. This is part of a 97-day periodicity due to stellar rotation, derived by Rivera et al. (2005), and confirmed by Sada's photometry concurrent with our observations. After removing the flare, we fit and remove the corresponding section of a 97-day sine wave, with amplitude scaled down to fit our time series data. Note that we expect more muted changes due to stellar rotation at this long IR wavelength as compared to visible wavelengths. Based on temperatures for starspots in active late-type stars (Strassmeier & Olah 1992), Sada's 2.0 mmag per day at Johnson *B* scales to 0.8 mmag per day at  $8 \mu\text{m}$ , in good agreement with our observed slope. This gradual decline in stellar brightness is a more serious problem than the stellar flare for putting limits on the planet signal, as explained in the following section.

The middle panel of Figure 1 shows the data after removal of the stellar and linear baseline in units of the average stellar brightness. The scatter per point is  $3.9 \times 10^{-4}$ , only slightly larger than the photon noise ( $3.54 \times 10^{-4}$ ). We thus obtain about 90% of the photon-limited signal-to-noise ratio. The distribution of photometric values (Figure 1, middle panel) after removal of stellar effects is indistinguishable from Gaussian. Under our hypothesis of a planet lacking an atmosphere, the flux modulation due to the planet should peak at phase 0.5, computed from the ephemeris values given by Rivera et al. (2005) and updated by E. J. Rivera and G. Laughlin (2008, private communication). However, we point out that removal of the baseline slope will affect the extraction of a planet signal, since the partial sine wave due to the planet has a component in common with a linear baseline. To account for this effect, we fit and remove a straight line from the planet model, and we fit the difference curve (a "reduced sine") to the data in order to estimate the best-fit planet amplitude and error.

A least-squares fit of a reduced sine wave peaking at phase 0.5 gives an amplitude of  $1.26 \pm 1.71 \times 10^{-5}$ , i.e., zero within the errors. To determine the error, we fit similar reduced sine waves to 100,000 bootstrap Monte Carlo trials based on permutations of Figure 1 (middle panel) data. Tabulating the distribution of sine wave amplitudes from these trials, we find an excellent fit to a Gaussian distribution, with a  $3\sigma$  limit =  $5.13 \times 10^{-5}$ . From the photometric calibration of our data, we find the flux from the star to be 864 mJy, so our  $3\sigma$  limit on the amplitude due to the planet is  $44 \mu\text{Jy}$ . At a 99% confidence level, the flux modulation limit due to the planet is  $34 \mu\text{Jy}$ . To illustrate the  $3\sigma$  limit in a "chi-by-eye" fashion, the lower panel shows a sine wave with

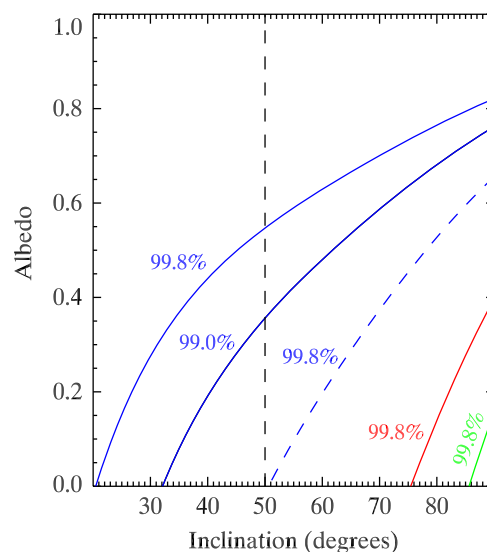


**Figure 2.** Inclinations and albedos for which an atmosphere can be inferred. Each line is the locus of orbit inclination and albedo values that would produce an  $8 \mu\text{m}$  sinusoidal flux modulation corresponding to our 99.8% and 99.0% confidence upper limits ( $44$  &  $34 \mu\text{Jy}$ ). Color encodes planet composition: pure water ice planets (solid blue curve); "dirty" ocean planets (dashed blue curve, 6.5% by mass iron core, 48.5% silicate mantle, and 45% ice outer layers, or different combinations with the same mass and radius); an Earth-like composition (red curve, 32.5% iron core and 67.5% silicate mantle); and a Mercury-like composition (green curve, 70% iron core and 30% silicate mantle). A GJ 876 with no atmosphere is allowed by our data above each line; the regions below the line are forbidden at that confidence level. In other words, if GJ 876d has a composition, orbit inclination, and albedo lying in the regions below the curves, then we would infer the presence of an atmosphere.

(A color version of this figure is available in the online journal.)

$44 \mu\text{Jy}$  amplitude in comparison to our data binned into eight phase intervals, as well as the nominal best-fit amplitude (not a detection).

#### 4. RESULTS

Our *Spitzer* 32-hr data set shows no evidence for the sinusoidal variation peaking at phase 0.5. To interpret the observed limit on flux modulation, we need to account for the orbit inclination of the planet and the albedo. We assume a tidally locked rotation with no heat redistribution, because we are testing the no-atmosphere hypothesis. At each assumed inclination value, we compute the thermal radiance curve of the planet, emitting as a Lambertian sphere. Given an assumed inclination, the Doppler data yield a mass, and we compute a radius for various compositions using the mass-radius relationships calculated by Seager et al. (2007). This information is sufficient to define the amplitude of the planet's thermal emission curve at all values of orbit inclination and albedo (see Equation (8)).

A given upper limit on the planet thermal phase curve corresponds to a locus of values in the inclination-albedo space illustrated in Figure 2. Tidally locked atmosphereless planets with albedos and inclinations in the regions below the curves in Figure 2 would have high enough thermal phase curve amplitudes to be detected, and are therefore ruled out by our observations. In other words, if for a given composition GJ 876d has an albedo and inclination such that it lies below an upper limit curve in Figure 2, we could infer the presence of an atmosphere (implying efficient heat redistribution between the tidally locked planet's day and night side). We emphasize again that the observations actually rule out combinations of

inclination, albedo, and *radius*. By knowing GJ 876d's mass at a given inclination, we can translate a mass and adopted interior composition to a radius, using planet interior models.

We are able to make robust (99.8% confidence level) upper limit statements that are inclination-, albedo-, and composition-dependent, corresponding to regions below the curves in Figure 2. As an example, we would infer the presence of an atmosphere if GJ 876d is a pure water ice planet that has an albedo less than 0.35 if the planet's orbital inclination is  $50^\circ$  (the inferred inclination from Rivera et al. 2005). We would infer the presence of an atmosphere for a planet with the same composition and an albedo less than 0.79 and an inclination of  $84^\circ$  (the inferred inclination from Benedict et al. 2002). A pure water ice planet is not a particularly useful example because planets are expected to have some rocky component. We can also infer the presence of an atmosphere if GJ 876d is less dense than a planet with Earth's bulk composition (approximately 32.5% iron core and 67.5% silicate perovskite mantle) and has a geometric albedo less than 0.25 and an inclination of  $84^\circ$ . Because a bare rocky planet likely has an albedo lower than 0.25, we would infer the presence of an atmosphere on GJ 876d for this composition and inclination. For other albedo/inclination values for which we could infer the presence of an atmosphere for a given hypothetical composition of GJ 876d, see the curves in Figure 2. We are unable to make conclusive statements about planets more dense than those with Earth's composition, because size decreases with increasing density, and smaller sized planets would have a smaller thermal phase variation, rendering them undetectable in our data.

## 5. DISCUSSION

We reported nearly continuous 32 hr of Spitzer IRAC data of GJ876d. The goal was to infer whether or not GJ 876d has an atmosphere, because a tidally locked planet with no atmosphere is expected to show a Lambertian-like thermal phase curve. We are unable to either conclusively infer the presence of an atmosphere or rule one out. We can present inclination- and albedo-dependent statements of what kind of planet atmospheres are ruled out if GJ876d is a planet of relatively low average density for a solid planet (see Figure 2).

The limiting factor in our data analysis is variation of the stellar flux. The presence of a slow linear drift increases the size of an atmosphereless planet that can hide in the data. Even though GJ 876d is a quiet M star, it still shows variability on a rotational time scale of 96.7 days (Rivera et al. 2005).

The serendipitous detection of a flare (Figure 1) is further evidence for activity on a very slightly active star. We emphasize that the flare itself should not impede efforts to extract the planet signal, because the flare has a specific shape and a relatively short duration. The detection of infrared microflares on M stars may provide a new way to study M star activity not available from the ground.

Ground-based visible photometric monitoring of the star during the IR space-based measurements, combined with the rotation rate of the star and a star spot model (area and temperature of spots) would help to subtract any stellar variability in the light curve. Additionally, space-based IR monitoring before and after the planet observations would extend the data baseline to help precisely define the stellar variability. Future observations should also use continuous observations of the planet–star system, not just for maximizing S/N, but also to avoid the detrimental “ramp” effects that would be caused by observations of other targets of random brightnesses. Monitoring of a planet

over two or more orbital periods would also help disentangle a linear stellar variability component.

Higher S/N would also mitigate effects of stellar variability. Our upper limit was degraded because of the overlap between a component of the planet's variation and the stellar variability. We fit to the data with a “degraded template.” Having more photons would help us to get more precision, and tighter limits than using such a degraded template. We caution that with more photons we might encounter another aspect of stellar variability at a lower level. Our observations may be the first to indicate the difficulty even low levels of stellar variability have on observational studies in the combined light of the planet and star, for any kind of exoplanets orbiting an M star.

Knowing the inclination of GJ 876d would help in interpreting our data. Rivera et al. (2005) provide an inclination for the GJ 876 3-planet system of  $\sim 50^\circ$ , based on stability arguments for the two  $\sim$ Jupiter-mass planets GJ 876b and GJ 876c, assuming that the lower mass GJ 876d is also coplanar. *Hubble Space Telescope* Fine Guidance Sensor observations (Benedict et al. 2002), in contrast to the theoretical simulations, give an inclination of GJ 876b of  $84^\circ \pm 6^\circ$ . Even with improved observations and theoretical simulations, the inclination of GJ 876d may remain unknown, unless we adopt the dynamical assumption that it should be coplanar with its more massive planet siblings.

Transiting planets provide a much better opportunity for observations to infer whether or not an atmosphere exists from a thermal phase curve compared to a planet with unknown orbital inclination. Because a transiting planet's orbital inclination is near  $90^\circ$ , the planet–star flux contrast is maximized for a bare rock planet. The radius of a transiting planet is known, enabling a specification of the albedo without resort to mass–radius interior models. (While non-transiting planets with known inclination would still help with interpreting the results, the unknown radius remains a complicating factor.) We can use Figure 2 to understand what kind of limits one could put for comparable data for a transiting planet. If GJ 876d were a transiting planet at  $90^\circ$  inclination with no evident thermal phase variation, we would infer an atmosphere on GJ 876d for almost any interior composition. The exception is planets denser than a planet with a Mercury-like interior composition (approximately 70% iron core and 30% silicate mantle); slightly higher S/N data would be needed. For a planet with a Mercury-like composition, the albedo upper limit is 0.15. Most bare rocky bodies in our solar system have albedos lower than this value (Mercury's geometric albedo is 0.1 and the Moon's is 0.12). One exception is Io, Jupiter's atmosphereless moon, with a high geometric albedo (0.63, Cox 2000) due to fresh solid sulfur deposits from episodic volcanic outbursts, themselves caused by tidal friction with Jupiter. Although many of the icy satellites of the outer planets also have very high geometric albedos (0.63, Cox 2000), an ice-covered surface is not expected for hot planets like GJ 876d and others at very close planet–star separations. Data with S/N  $\sim 3$  times higher than our data set reported here would rule out such high albedos even for the smallest plausible planets.

We have discussed how to infer the presence of an atmosphere on an exoplanet. Can an atmosphere be ruled out based on detection of a thermal phase curve? In principle, a planet with a thick atmosphere having inefficient heat redistribution (e.g., Harrington et al. 2006) could produce a signal similar to a bare rock. Measuring the phase of the orbit variation to high precision is needed; a bare rock must peak very close to phase 0.5, but a planet with a thick atmosphere should have a detectable phase

shift of the thermal maximum, even for relatively inefficient heat transport. Discriminating between a planet with a very thin atmosphere and a bare rock may be more difficult, and requires further study.

Observation of the combined light of the planet and star as a function of phase may also reveal the presence of a relatively strong planetary magnetic field. For short-period planets, the planet and star magnetic fields could interact to produce a phase curve peaking at phases near  $180^\circ$  with a period equal to that of the planet's orbit, as has been detected for a few hot Jupiters (Shkolnik et al. 2005; Donati et al. 2008; Shkolnik et al. 2008). The question of super Earth magnetic fields is a serious one. Without a protective magnetic field the atmosphere might be further eroded by stellar wind and high energy particles. A detection of a relatively strong magnetic field would indicate the presence of a partially liquid interior, aiding interpretation of interior composition (and even further interesting for short-period planets under strong tidal interaction).

We note that Mercury is not tidally locked to the Sun, (i.e., in a 1:1 resonance). Instead Mercury is in a 3:2 resonance, and rotating 3 times for every two orbits about the Sun. Models show a low probability for a planet on a circular orbit to become trapped in the 3:2 spin-orbit resonance compared to the 1:1 resonance, unless it goes through a chaotic evolution of an eccentric orbit as Mercury likely has (Correia & Laskar 2004). Planets on circular orbits are therefore more certainly tidally locked than eccentric planets which may have had the opportunity of being captured into higher order spin-orbit resonances.

The *James Webb Space Telescope (JWST)*, with its 58 times more collecting area than *Spitzer* will be able to make high S/N observations of short-period super Earths. M stars are good targets, because they are bright at IR wavelengths and the planet-star radius ratio is high.

In conclusion, inferring an atmosphere on a short-period, tidally locked super Earth that lacks a thermal phase curve is possible for a transiting planet of any interior composition and albedo, provided that the data set has higher S/N by about a factor of 3 than ours. During the *JWST* era, we anticipate the birth of studies of atmosphereless bodies and the concomitant understanding of atmospheric escape.

We thank Feng Tian, Andrew West, Brad Hager, Leslie Rogers, and Lindy Elkins-Tanton for many useful discussions. We thank Eugenio Rivera and Greg Laughlin for providing an unpublished updated ephemeris for GJ 876d, Pedro Sada for communicating his GJ 876 photometry in advance of publication, and Heather Knutson for showing us her unpublished photometry of the M dwarf companion to 189733. We thank an anonymous reviewer for a careful read of our paper. We thank the *Spitzer* Science Center staff for their efficient scheduling of our observations and for assistance in finding the best pre-

flash source. This work is based on observations made with the *Spitzer Space Telescope*, which is operated by the Jet Propulsion Laboratory, California Institute of Technology under a contract with NASA. Support for this work was provided by NASA through an award issued by JPL/Caltech.

## REFERENCES

- Baglin, A. 2003, *Adv. Space Res.*, **31**, 345  
 Benedict, G. F., et al. 2002, *ApJ*, **581**, L115  
 Bonfils, X., et al. 2007, *A&A*, **474**, 293  
 Borucki, W. J., et al. 2003, *Proc. SPIE*, **4854**, 129  
 Butler, R. P., Vogt, S. S., Marcy, G. W., Fischer, D. A., Wright, J. T., Henry, G. W., Laughlin, G., & Lissauer, J. J. 2004, *ApJ*, **617**, 580  
 Charbonneau, D., Noyes, R. W., Korzennik, S. G., Nisenson, P., Jha, S., Vogt, S. S., & Kibrick, R. I. 1999, *ApJ*, **522**, L145  
 Cockell, C. S., et al. 2009, *Astrobiology*, **9**, 1  
 Correia, A. C. M., & Laskar, J. 2004, *Nature*, **429**, 848  
 Cowan, N. B., Agol, E., & Charbonneau, D. 2007, *MNRAS*, **379**, 641  
 Cox, A. N. 2000, *Allen's Astrophysical Quantities* (New York: Springer)  
 Deming, D., Harrington, J., Seager, S., & Richardson, L. J. 2006, *ApJ*, **644**, 560  
 Donati, J.-F., et al. 2008, *MNRAS*, **385**, 1179  
 Elkins-Tanton, L. T., & Seager, S. 2008, *ApJ*, **685**, 1237  
 Endl, M., & Kürster, M. 2008, *A&A*, **488**, 1149  
 Gaidos, E., & Williams, D. M. 2004, *New Astron.*, **10**, 67  
 Goldreich, P., & Soter, S. 1966, *Icarus*, **5**, 375  
 Harrington, J., Hansen, B. M., Luszcz, S. H., Seager, S., Deming, D., Menou, K., Cho, J. Y.-K., & Richardson, L. J. 2006, *Science*, **314**, 623  
 Harrington, J., Luszcz, S., Seager, S., Deming, D., & Richardson, L. J. 2007, *Nature*, **447**, 691  
 Knutson, H. A., et al. 2007, *Nature*, **447**, 183  
 Knutson, H. A., et al. 2009, *ApJ*, **690**, 822  
 Lammer, H., et al. 2007, *Astrobiology*, **7**, 185  
 Lawson, P. R., et al. 2008, *Proc. SPIE*, **7013**, 70132N  
 Lecavelier des Etangs, A. 2007, *A&A*, **461**, 1185  
 Leger, A., et al. 2009, arXiv:0908.0241  
 Maness, H. L., Marcy, G. W., Ford, E. B., Hauschildt, P. H., Shreve, A. T., Basri, G. B., Butler, R. P., & Vogt, S. S. 2007, *PASP*, **119**, 90  
 Mayor, M., et al. 2009, *A&A*, **493**, 639  
 Nutzman, P., & Charbonneau, D. 2008, *PASP*, **120**, 317  
 Reid, I. N., & Hawley, S. L. 2005, *New Light on Dark Stars: Red Dwarfs, Low-Mass Stars, Brown Stars* (New York: Springer)  
 Rivera, E. J., et al. 2005, *ApJ*, **634**, 625  
 Scalo, J., et al. 2007, *Astrobiology*, **7**, 85  
 Seager, S., Kuchner, M., Hier-Majumder, C. A., & Militzer, B. 2007, *ApJ*, **669**, 1279  
 Selsis, F. 2004, in ASP Conf. Ser. 321, *Extrasolar Planets: Today and Tomorrow*, ed. J. Beaulieu, A. Lecavelier Des Etangs, & C. Terquem (San Francisco, CA: ASP), **170**  
 Shankland, P. D., et al. 2006, *ApJ*, **653**, 700  
 Shkolnik, E., Bohlender, D. A., Walker, G. A. H., & Collier Cameron, A. 2008, *ApJ*, **676**, 628  
 Shkolnik, E., Walker, G. A. H., Bohlender, D. A., Gu, P.-G., & Kürster, M. 2005, *ApJ*, **622**, 1075  
 Sobolev, V. V. 1975, *Light Scattering in Planetary Atmospheres (Rasseianie sveta v atmosferakh planet, Moscow, Izdatel'stvo Nauka, 1972)* (Engl. Transl.; International Series of Monographs in Natural Philosophy., Vol. 76; Oxford: Pergamon)  
 Strassmeier, K. G., & Olah, K. 1992, *A&A*, **259**, 595  
 Weis, E. W. 1994, *AJ*, **107**, 1135  
 West, A. A., Hawley, S. L., Bochanski, J. J., Covey, K. R., Reid, I. N., Dhital, S., Hilton, E. J., & Masuda, M. 2008, *AJ*, **135**, 785